Multilayer ceramic capacitors

66

Multilayer Ceramic Capacitor

- The demands for miniaturization largely preclude an increase in the face area A.
- One exception is the multilayer ceramic capacitor (MLCC), in which case:

$$C = \varepsilon_r \varepsilon_o \frac{A(N-1)}{d}$$

- where N is the number of stacked plates.
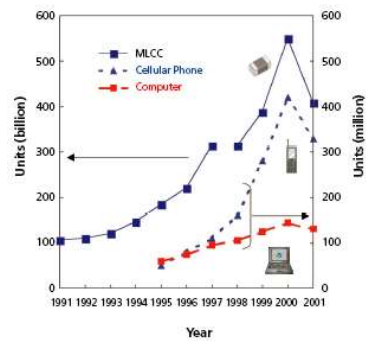- Ideally, the dielectric should have a low electrical conductivity so that the leakage current is not too large.

67

Multilayer Ceramic Capacitor

Multi Layer Ceramic Capacitor (MLCC)

http://www.btu.com/images/smt_epp.jpg

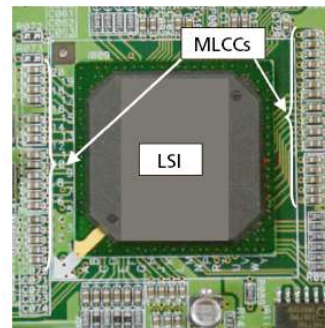$$C = \varepsilon_0 \varepsilon_r \frac{A}{d}$$
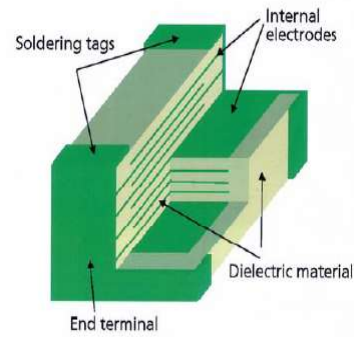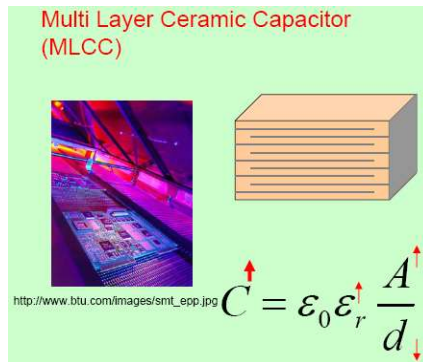
Cut-away view of multilayer ceramic capacitor.
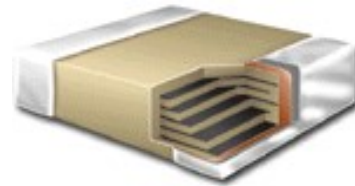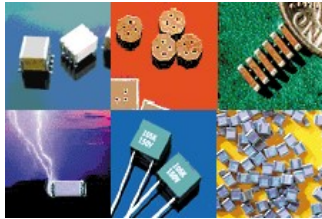
68

Change in production volume of MLCCs in the world

Example of MLCC application in LSI circuit.

69

2

Surface-Mount Ceramic Capacitors

Military electronics

70

Surface-Mount Capacitors

- Ceramic surface-mount capacitors are used in every type of electronic equipment including computers, telecommunication, automotive electronics, military electronics, medical electronics and consumer electronics.

- High voltage and high temperature ceramic capacitors are serve military, aerospace, oil service, oil exploration and other markets including medical imaging, power generation, and high voltage power supply.

https://www.electronics-notes.com/articles/electronic_components/capacitors/smd-smt-surface-mount-capacitor.php

71

Multilayer ceramic capacitors

Ceramic

Termination

Termination
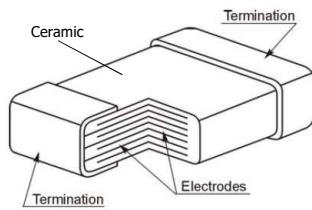
Electrodes

A surface-mount (chip) MLC.

MLCC: *n* ceramic layers of thickness *d* separated by metal (Ni, Ag-Pd) electrodes.
Capacitance per unit volume:

$$C_V = \varepsilon_r \frac{n}{d^2}$$

Current market trends:
- increase capacitance (increase *n* and decrease *d*)
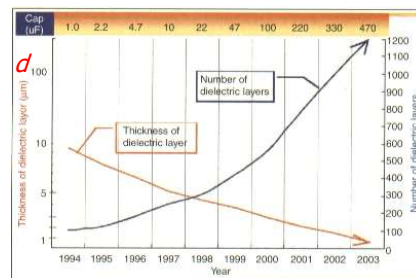- miniaturization (reduce *d* and size)

$$C = \varepsilon_r \varepsilon_o \frac{A(N-1)}{d}$$

d

n

72

Multilayer ceramic capacitors

Some data

❑ Main dielectric material: $BaTiO_3$. Yearly production: 11000 tons → 2×10^{12} MLCCs (2011);

❑ Dielectric properties are modified by adding dopants (Zr, Ca, Mg, Nb, Y, Ho, Dy, etc.);

❑ State of the art capacitors: dielectric layer thickness of 0.5 micron (Murata, Japan);

❑ Production technology: tape casting;

❑ Metal electrodes:

  - Noble metals: Ag-Pd, sintering in air with addition of glass to reduce temperature to 1100°C (Ag-30Pd);

  - Ni (base metal technology, Philips, 1990s): sintering in N_2-H_2 atmosphere. Addition of "magic" dopants (Y, Dy, Ho) to reduce formation of oxygen vacancies and improve lifetime.

❑ Applications: consumer electronics (mobile phones, smart phones, PCs, laptops, TVs, etc.), automotive (cars, hybrid cars, electric vehicles).

d=0.5 µm

State-of-the-art MLCC:
d = 0.5 µm → *gs* ≈100 nm

73

4
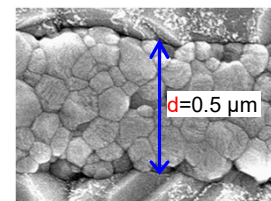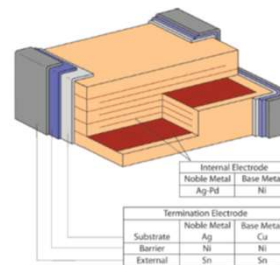
Multilayer ceramic capacitors

MLCCs fabrication process (multilayer cofire technology)
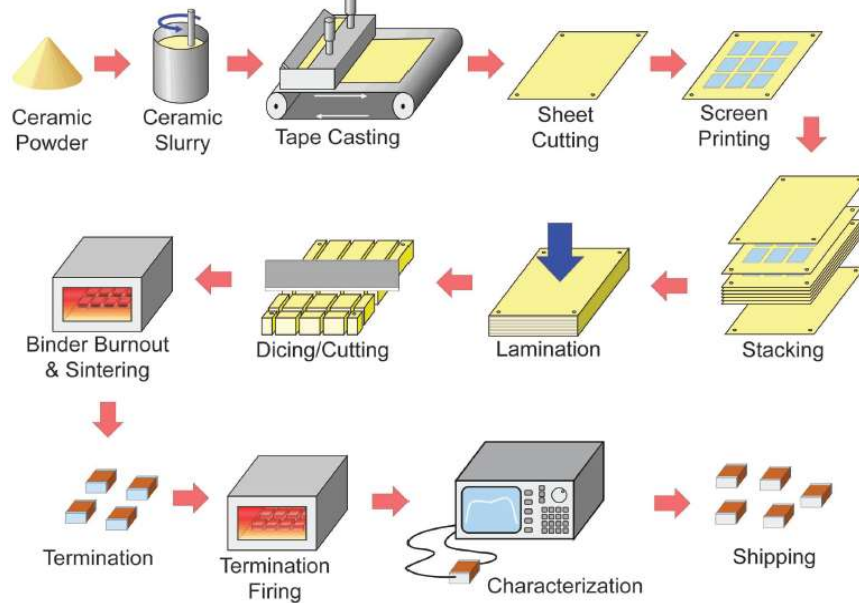
74

Multilayer ceramic capacitors

A surface-mount (chip) MLC.

Metal electrode

Dielectric ceramic layer at least 5-7 grains
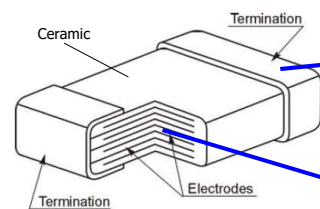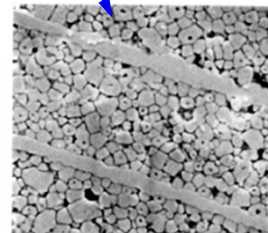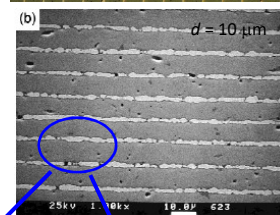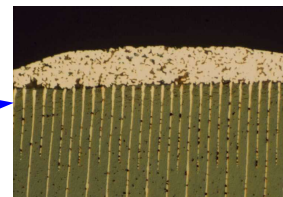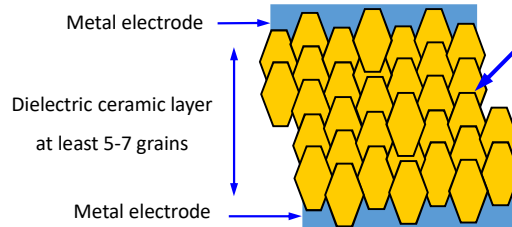
Metal electrode

d = 10 μm

75

Multilayer ceramic capacitors

Miniaturization

muRata

External view and dimensions

Part Number	Dimensions (mm)				
	L	W	T	e	g min.
GRM022	0.4 ±0.02	0.2 ±0.02	0.2 ±0.02	0.07 to 0.14	0.13
GRM033	0.6 ±0.03	0.3 ±0.03	0.3 ±0.03	0.1 to 0.2	0.2
GRM15X	1.0 ±0.05	0.5 ±0.05	0.25 ±0.05	0.1 to 0.3	0.4
GRM153			0.3 ±0.03		
GRM155			0.5 ±0.05	0.15 to 0.35	0.3
GRM185	1.6 ±0.1	0.8 ±0.1	0.5 +0/-0.1	0.2 to 0.5	0.5
GRM188*			0.8 ±0.1		
GRM216	2.0 ±0.1	1.25 ±0.1	0.6 ±0.1	0.2 to 0.7	0.7
GRM219			0.85 ±0.1		
GRM21A			1.0 +0/-0.2		
GRM21B			1.25 ±0.1		
GRM316	3.2 ±0.15	1.6 ±0.15	0.6 ±0.1	0.3 to 0.8	1.5
GRM319			0.85 ±0.1		
GRM31M			1.15 ±0.1		
GRM31C	3.2 ±0.2	1.6 ±0.2	1.6 ±0.2		
GRM329	3.2 ±0.3	2.5 ±0.2	0.85 +0.15/-0.05	0.3 min.	1.0
GRM32A			1.0 +0/-0.2		
GRM32M			1.15 ±0.1		
GRM32N			1.35 ±0.15		
GRM32C			1.6 ±0.2		
GRM32R			1.8 ±0.2		
GRM32D			2.0 ±0.2		
GRM32E			2.5 ±0.2		

* Bulk Case: 1.6 ±0.07(L)✕0.8 ±0.07(W)✕0.8 ±0.07(T)

Form Factor	Dimensions (mm)		
	L	W	T
C1005	1.00 ±0.05	0.50 ±0.05	0.50 ±0.05
C1608	1.60 ±0.10	0.80 ±0.10	0.80 ±0.10
C2012	2.00 ±0.20	1.25 ±0.20	1.25 ±0.20
C3216	3.20 ±0.20	1.60 ±0.20	1.60 ±0.20
C3225	3.20 ±0.30	2.50 ±0.30	2.50 ±0.30

d=0.5 µm

State-of-the-art MLCC:
d = 0.5 µm → *gs* ≈100 nm

76

High-K Dielectric Materials

- The discovery of materials with unusually high-dielectric constants (ε_r > 2000-100000), and their ferroelectric nature, led to an explosion in ceramic use.

- The first employed in high-k capacitors is BaTiO$_3$ based, and later developed into
  - *piezoelectric transducers,*
  - *positive temperature coefficient (PTC) devices, and*
  - *electro-optic light valves.*

- Recent developments in the field of ferroelectric ceramics is their use in
  - *medical ultrasonic composites,*
  - *high displacement piezoelectric actuators, and*
  - *photoresistors.*

77

High-K Dielectric

- The bit count of MOS DRAM devices is continuously increasing. However, as bit count goes up, capacitor cell area goes down.

- The capacitance per cell must remain in the 25-30 fF range, which means the capacitance density must increase.

- One approach for DRAM manufacturing is to replace the traditional silicon nitride + silicon oxide with a higher dielectric constant (k) such as tantalum pentoxide (Ta_2O_5), Hf-oxide (HfO_2) and Zr-oxide (ZrO_2).

78
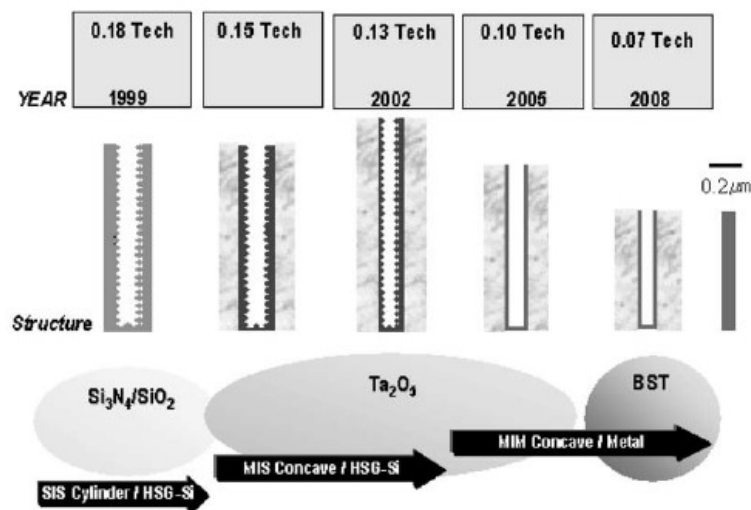
The roadmap of capacitor with DRAM technology.

79

High-K Dielectric

- High-k dielectric films are anticipated to be required for certain applications with low power and leakage current specifications.
- High-k materials should be compatible with conventional industry standard MOSFET process flows using a poly-Si gate electrode.
- HfO_2, ZrO_2, and Ta_2O_5 as high-k gate-dielectrics.

80

Typical material stack used in aTa_2O_5 DRAM capacitor
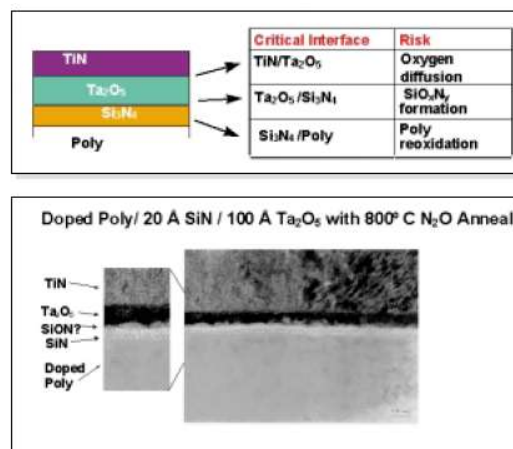
81

A Review of High High-k Dielectrics

- Gate dielectric materials having high dielectric constant, large band gap with a favorable band alignment, low interface state density and good thermal stability are needed for future gate dielectric applications.
- Ultra high-k materials such as STO ($SrTiO_3$) or BST ($BaSrTiO_3$) may cause fringing field induced barrier lowering effect.
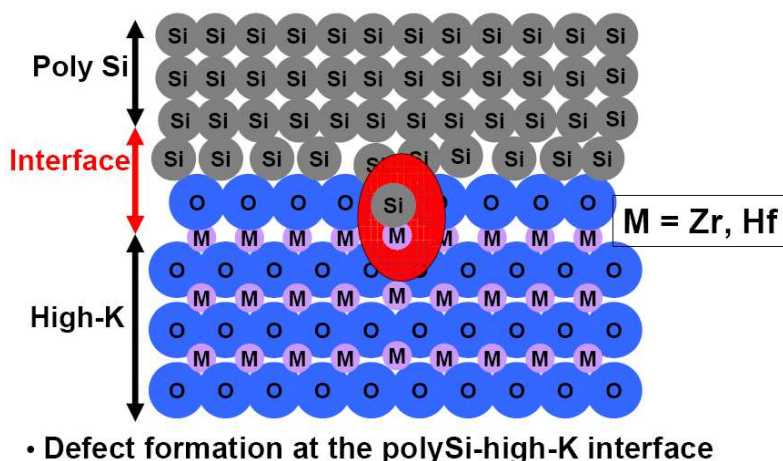
82

A Review of High High-k Dielectrics

- High-k gate dielectrics have a number of difficulties:

  (1) crystallization upon heating,

  (2) dopant penetration,

  (3) fixed charge,

  (4) low channel mobility and

  (5) uncontrolled oxide formation at the Si/high-k interface.

83

High-K and PolySi are Incompatible

Poly Si

Interface

High-K

M = Zr, Hf

• Defect formation at the polySi-high-K interface
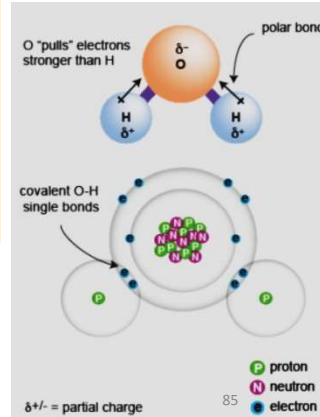
84

Water and microwaves

Unlike conventional ovens, microwave ovens do not rely on temperature gradients (outside to inside) for heat transfer but involve penetrative and instantaneous heating. The microwave oven is part of modern life, **but how do the microwaves interact with water in food to efficiently heat the food?**

Non-equilibrium molecular dynamics simulations have been used to investigate the hydrogen-bond dynamics in bulk water upon microwave heating [1]. The water dipole attempts to continuously reorient in electromagnetic radiation's oscillating electric field. Dependent on the frequency, the dipole may move in time to the field, lag behind it or remain apparently unaffected. *When the dipole lags behind the field, interactions between the dipole and the field lead to an energy loss by heating, which depends on the phase difference of these fields; heating is maximal twice each cycle* [2].

The ease of the movement depends on the viscosity and the mobility of the electron clouds. In water, these rely on the strength and extent of the hydrogen-bonded network. **In free liquid water, this movement occurs at GHz frequencies (microwaves), whereas in more restricted 'bound' water it occurs at MHz frequencies (short radio waves) and in ice at kHz frequencies (long radio waves).** The re-orientation process may be modeled using a 'wait-and-switch' process where the water molecule has to wait for a while until a favorable orientation of neighboring molecules occurs, and then the hydrogen bonds switch to the new molecule [3].

1.   T. Mohoriĉa and U. Brena, How does microwave irradiation affect the mechanism of water reorientation? Journal of Molecular Liquids, 302 (2020) 112522
2.   N. J. English and J. M. D. MacElroy, Molecular dynamics simulations of microwave heating of water, Journal of Chemical Physics,118 (2003) 1589-1592
3.   U. Kaatze, R. Behrends and R. Pottel, Hydrogen network fluctuations and dielectric spectrometry of liquids, Journal of Non-Crystalline Solids, 305 (2002) 19-28
4.   https://www.nature.com/articles/293447a0 [Theory of the dielectric constant of ice, David J. Adams, Nature volume 293, pages447–449 (1981)]
https://water.lsbu.ac.uk/water/ [London South Bank Univ. page]

polar bond

O "pulls" electrons stronger than H

δ- O

H δ+   H δ+

covalent O-H single bonds

δ+/- = partial charge

P proton
N neutron
electron

85

The applied field potential (E, volts) of electromagnetic radiation is given by;

$$E = E_{max}.\cos(\omega t)$$

where E_{max} is the amplitude of the potential, ω is the angular frequency in radians.second^{-1}, and t is the time (seconds). If the polarization lags behind the field by the phase (δ, radians) then the polarization (P, coulombs) varies as

$$P = P_{max}.\cos(\omega t - \delta)$$

where P_{max} is the maximum value of the polarization.
Hence the current (I, amperes) varies as

$$I = (dP/dt) = -\omega P_{max}.\sin(\omega t - \delta)$$

The power (***P***, watts) given out as heat is the average value of (current × potential). This is zero if there is no lag (that is, if δ = 0), otherwise

$$\boldsymbol{P} = 0.5\ P_{max}E_{max}\omega.\sin(\delta)$$

Lagging cosine wave of the resultant polarisation

electric field E

resulting polarisation P

←δ→
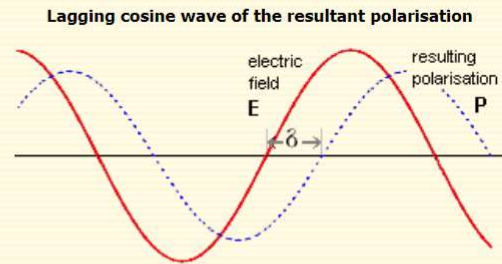
86

Ferroelectric ceramics

87

Classification of Dielectrics

One can classify dielectric as under following three groups:

Class	Effect of electric field
Simple dielectrics	Creates dipoles
Paraelectrics	Orients dipoles
Ferroelectrics	Orients domains of aligned permanent dipoles

Properties of some representative ferroelectric crystals

Group	Crystal	Curie temperature T_c (°K)	P_s $C/m^{-2} \times 10^{-2}$	At T (°K)
Ilmenites and Perovskites	GeTe	670	—	—
	$LiNbO_3$	1480	71	296
	$KNbO_3$	710	30	600
	$BaTiO_3$	393	26	300
	$SrTiO_3$	32	3	4.2
KDP type	KH_2PO_4 (KDP)	123	4.7	100
	KD_2PO_4	213	5.5	100
	$Rb_2H_2PO_4$	147	5.6	90
	KH_2AsO_4	97	5.0	78
TGS type	$(NH_2CH_2COOH)_3 \cdot H_2SO_4$ (Triglycine sulphate)	322	2.8	275
Rochelle salt type	$NaKC_4H_4O_6 \cdot 4H_2O$ (Rochelle salt)	296 (upper) 255 (lower)	0.25	275

88

Important events in the history of ferroelectrics

|	
1824	Pyroelectricity in Rochelle salt $NaKC_4H_4O_6*4H_2O$ (Brewster)
1880	Piezoelectricity in quartz and Rochelle salt (Jacques & Pierre Curie – quartz balance)
1912	Ferroelectricity proposed as a property of solids
1921	Ferroelectricity in Rochelle salt (Valasek)
1935	Ferroelectricity in KH_2PO4
1941	**High dielectric constant in $BaTiO_3$**
1944	**Ferroelectricity in $BaTiO_3$ (von Hippel, Wul & Goldman)**
1945	**$BaTiO_3$ ceramics for piezoelectric transducers (electrical poling)**
1949	Theory of ferroelectricity in $BaTiO_3$ (Devonshire)
1949	Ferroelectricity in $LiNbO_3$ and $LiTaO_3$
1952	**Phase diagram of $Pb(Zr,Ti)O_3$ – PZT established**
1954	PZT reported as a useful piezo transducer
1955	Ferroelectricity in alkali niobates
1961	**$PbMg_{1/3}Nb_{2/3}O_3$-PMN reported as ferroelectric relaxor**
1969	Optical transparency achieved in hot pressed PLZT
1971	Useful electrooptical properties reported for PLZT
1980	Electrostrictive PMN devices developed
1992	New types of PZT piezo actuators developed
1993	**Integration of FE films on silicon technology - FERAMs**
1997	Ultrahigh piezoelectric coefficients in PMN-PT and PZN-PT
2002	**High polarization and magnetoelectric coupling in $BiFeO_3$ films**
2004	High-performance lead free KNN piezoceramics ($K_xNa_{1-x}NbO_3$)

89

Ferro & Piezoelectrics: Key Points
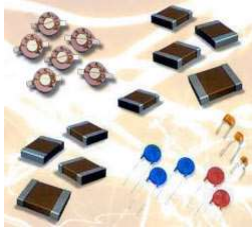
Ceramic capacitors

Flash Goggles, PLZT
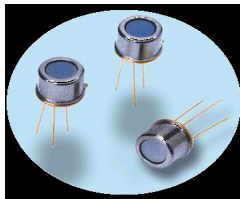
Infrared sensors

Piezoelectric Materials

- Ferroelectrics: materials with non-centrosymmetry, having (electrically) re-orientateable spontaneous polarisation at equilibrium.

- **Piezoelectricity: material property that linearly relates applied stresses to induced dielectric displacements (direct effect) or applied electric fields to induced strains (converse effect)**

- Popular examples: $BaTiO_3$ and Lead zirconate titanate (PZT); Lead -free compositions of Sodium potassium niobate (NKN)

90

Important events in the history of ferroelectrics

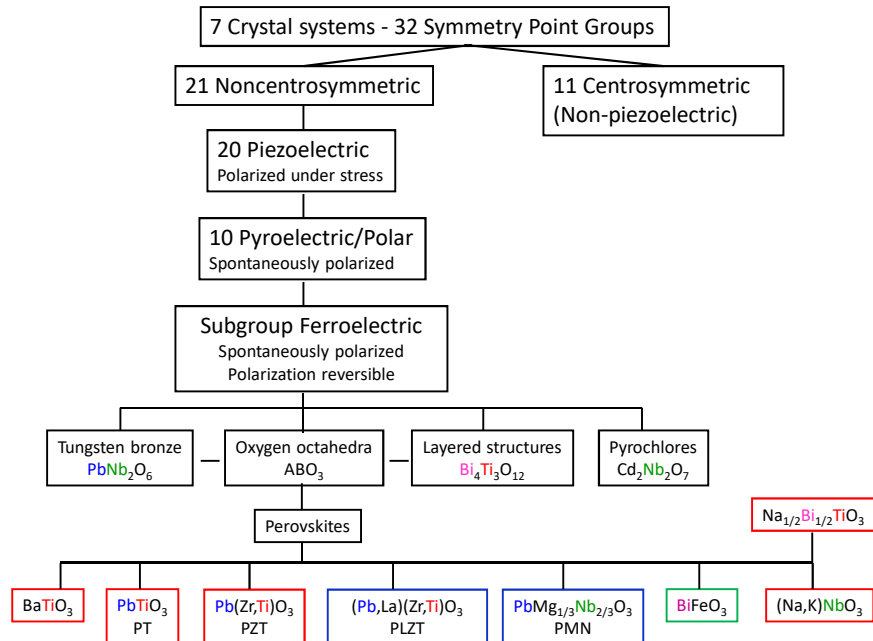Fundamental steps in the understanding and application of ferroelectric and piezoelectric ceramics

(1) The discovery of unusually high dielectric constant of $BaTiO_3$ (→ multilayer ceramic capacitors - MLCCs).

(2) The discovery that the origin of the high dielectric constant in $BaTiO_3$ is its ferroelectric nature, thus disclosing an entire new class of piezoelectric/ferroelectric materials –ABO_3 perovskites with BO_6 octahedra. Ferroelectricity no longer related to hydrogen bonds.

(3) The discovery of the electrical poling process to align the electrical dipoles of the grains/domains within the ceramics obtaining properties similar to those of single crystals (large scale production and application of piezoelectric transducers and actuators).
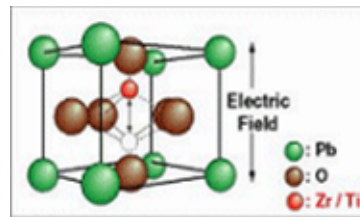
91

Piezoelectricity and ferroelectricity in solids

```
        ┌─────────────────────────────────────────┐
        │ 7 Crystal systems - 32 Symmetry Point Groups │
        └─────────────────────────────────────────┘
              ┌────────────────┴────────────────┐
    ┌──────────────────────┐        ┌──────────────────────┐
    │ 21 Noncentrosymmetric │        │ 11 Centrosymmetric    │
    └──────────────────────┘        │ (Non-piezoelectric)   │
              │                      └──────────────────────┘
    ┌──────────────────────┐
    │ 20 Piezoelectric      │
    │ Polarized under stress│
    └──────────────────────┘
              │
    ┌──────────────────────┐
    │ 10 Pyroelectric/Polar │
    │ Spontaneously polarized│
    └──────────────────────┘
              │
    ┌──────────────────────┐
    │ Subgroup Ferroelectric│
    │ Spontaneously polarized│
    │ Polarization reversible│
    └──────────────────────┘
```

| Tungsten bronze $PbNb_2O_6$ | Oxygen octahedra ABO_3 | Layered structures $Bi_4Ti_3O_{12}$ | Pyrochlores $Cd_2Nb_2O_7$ |

$Na_{1/2}Bi_{1/2}TiO_3$

Perovskites

| $BaTiO_3$ | $PbTiO_3$ PT | $Pb(Zr,Ti)O_3$ PZT | $(Pb,La)(Zr,Ti)O_3$ PLZT | $PbMg_{1/3}Nb_{2/3}O_3$ PMN | $BiFeO_3$ | $(Na,K)NbO_3$ |

92

FERROELECTRIC CERAMICS

- This kind of material has perovskite structure, with general formula **ABO_3**, in which
  - A is a large divalent metal ion such as Pb^{2+} or Ba^{2+},
  - B is a small tetravalent metal ion, such as Ti^{4+} or Zr^{4+}, octahedrally coordinating with oxygen.
- Ferroelectricity occurs due to the displacement of positive ions B^{4+} and negative ions O^{2-} in opposite directions.

93

FERROELECTRIC CERAMICS
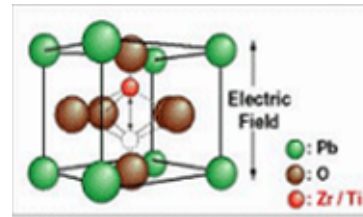
- This displacement causes *spontaneous polarisation* which is the origin of many other properties such as
  - extremely high dielectric constant,
  - hysteresis loop (non-linear dependence of polarisation with applied field),
  - piezoelectricity (the ability to change the dimension with applied field and to produce the current with applied mechanical stress).

94

FERROELECTRIC CERAMICS: PZT (PbZrTiO$_3$) structure
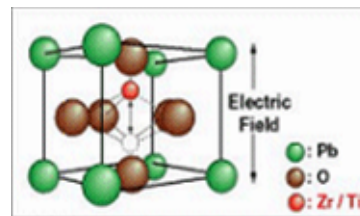
- Ferroelectric ceramics are widely used in modern technology with various applications (sensors, actuators, generators, transducers to very recent IC for RAM).

- They can be used for **DRAM** (dynamic random access memory), and high remanent polarisation and low coercive field for being used as **NVRAM** (non-volatile random access memory).
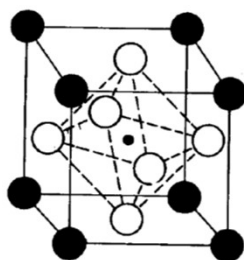
95

Structure of Barium Titanate (BaTiO₃)
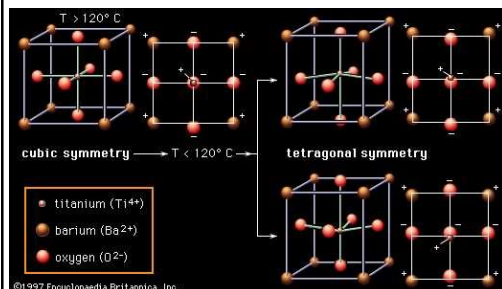
❖ **ABO$_3$** – General perovskite – **Cubic structure**
❖ O^{2-} (co-ordination 2) at Face centres and A^{2+} (co-ordination 12) at corner positions and B^{4+} (co-ordination 6) at body center.

Site	Co-ordinates
A cation	(0,0,0)
B cation	(½, ½, ½)
O anion	(½,½, 0) (½, 0, ½) (0, ½, ½)

Transitions in BaTiO₃

$$Cubic \xrightarrow{120\ ^\circ C} Tetragonal \xrightarrow{5\ ^\circ C} Orthorhombic \xrightarrow{-90\ ^\circ C} Rhombohedral$$
(Pm3m)　　　(P4mm)　　　(Amm2)　　　(R3m)

➢ BaTiO₃ – Centro symmetric with Ti^{4+} at body centre position with O^{2-} at face centres and Ba^{2+} at corner positions.
➢ Ti^{4+} occupies octahedral site as radius of Ti^{4+} is smaller than the radius of octahedral voids.
➢ Ti^{4+} ions shift from cube center when electric filed is applied resulting in high dielectric constant.
Ref: (Johnsson and Lemmens 2005)

Note: In BaTiO₃ cubic to tetragonal transition is a displacive transition (i.e., where atoms change its position in any one direction)

96

Tolerance factor of ABO$_3$ Perovskite – to estimate the degree of distortion

$$t = \frac{R_A + R_O}{\sqrt{2}(R_B + R_O)}$$

R_A = A – Cation ionic radius

R_B = B – Cation ionic radius

R_O = Oxygen Anion ionic radius

Ref: (Raengthon, McCue et al. 2016)

$$t = \frac{R_A + R_O}{\sqrt{2}(R_B + R_O)} * \frac{\Delta X(O - A)}{\Delta X(O - B)}$$

Modified Goldschmidt tolerance factor
$\Delta X(O - A)$ – Electronegativity difference b/w O and A
$\Delta X(O - B)$ - Electronegativity difference b/w O and B

Ref: (Brehm, Bennett et al. 2014)

Tolerance factor, t	Structure stability	Example	Reason/Remark
> 1	Hexagonal	BaNiO₃	A ion is too big
0.9 − 1	Cubic	BaTiO₃, SrTiO₃	Ideal sizes of A and B
0.71 − 0.9	Orthorhombic	CaTiO₃, GdFeO₃	B ion interstitial sites are large for A ions to fit
< 0.71	Polymorphs	FeTiO₃	Similar ionic sizes of A and B

Table Ref:
https://jaramillo.mit.edu/modified-goldschmidt-tolerance-factor-calculator-abx3-compounds

97

16

Polarization mechanisms – combination of ionic and dipole polarization causes ferroelectric properties in $BaTiO_3$ (Hoshina, Kigoshi et al. 2009)

❑ Ti^{4+} ions are small to be stable in octahedral site. It shifts to minimum energy positions along the direction of surrounded O^{2-} ions (i.e., along a single axis) (Richerson and Lee 2018)

- Ionic polarization – is due to Ba – O bonds. Atomic/ionic polarization tends to increase with temperature due to an increase in charge carriers and ion mobility.
- TiO_6 bonds – mixed covalent
- Spontaneous polarization – due to displacement of Ti^{4+} and O^{2-} ions in opposite directions thereby creating dipoles. These dipoles are retained even after the removal of applied voltage.

Non-centric atoms and their molecular orientations gives the retaining capacity for dipoles (Richerson and Lee 2018).
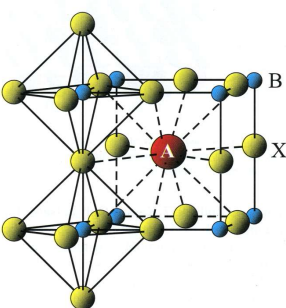
The ionic displacement in the c-axis direction initiates the ferroelectric dipole. Thus, it enhances the tetragonality (c/a) and creates large spontaneous polarization. However, there is an optimum oxygen pressure range to enhance the dielectric and ferroelectric of the $BaTiO_3$. With c-axis becoming relatively shorter, the dipole moment and the polarizability of the samples are reduced. **The c/a ratio of $BaTiO_3$ is 1.011 as per JCPDS (01-086-4991) and the lattice parameters are as follows: a = 3.9916 Å, c = 4.0363 Å**
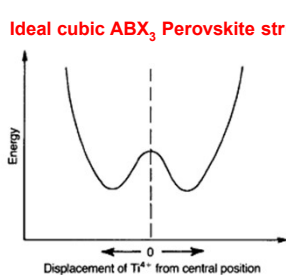
Extra Information:
- Molecular orientation polarization is only affected by low frequencies ($< 10^9$ Hz). In high frequency field, the molecules do not have time to realign with each cycle.
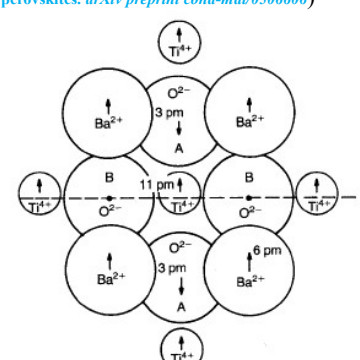- Electronic polarization occurs very rapidly and is present even at high frequencies (10^{15} Hz).

98

Atom positions in cubic Perovskites

Another way of representing $BaTiO_3$ – TiO_6 octahedron with O^{2-} vertices (Ti-O-Ti) edges and Ba^{2+} at cube centre (making Ba 12-fold co-ordination)

(Johnsson, M., & Lemmens, P. (2005). Crystallography and chemistry of perovskites. *arXiv preprint cond-mat/0506606*)
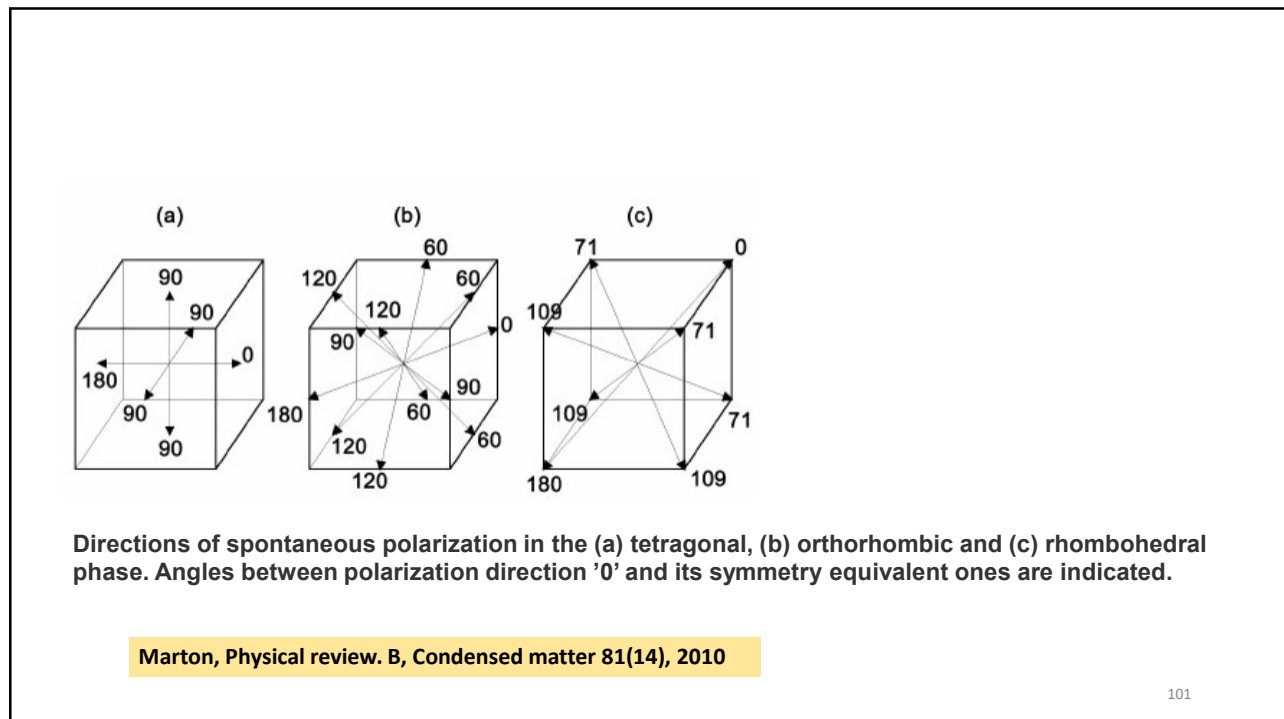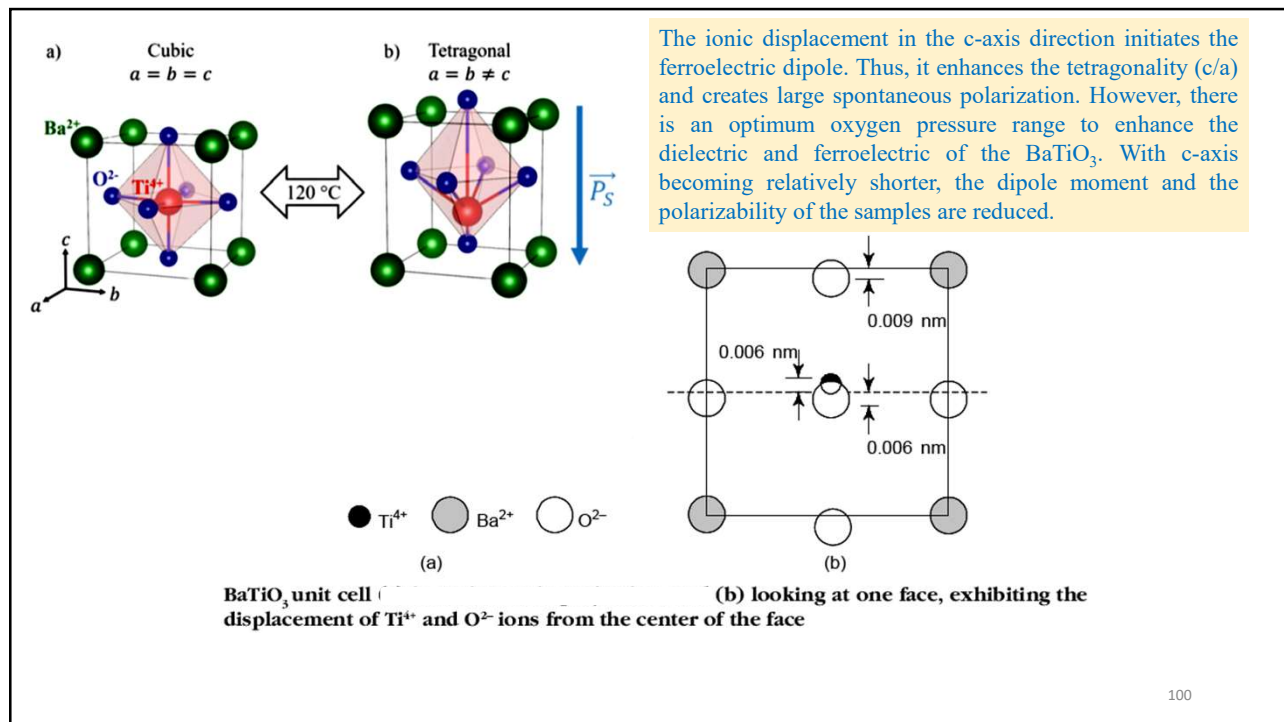

Ideal cubic ABX_3 Perovskite structure

Variation in the potential energy of Ti^{4+} along the c axis for Tetragonal BT
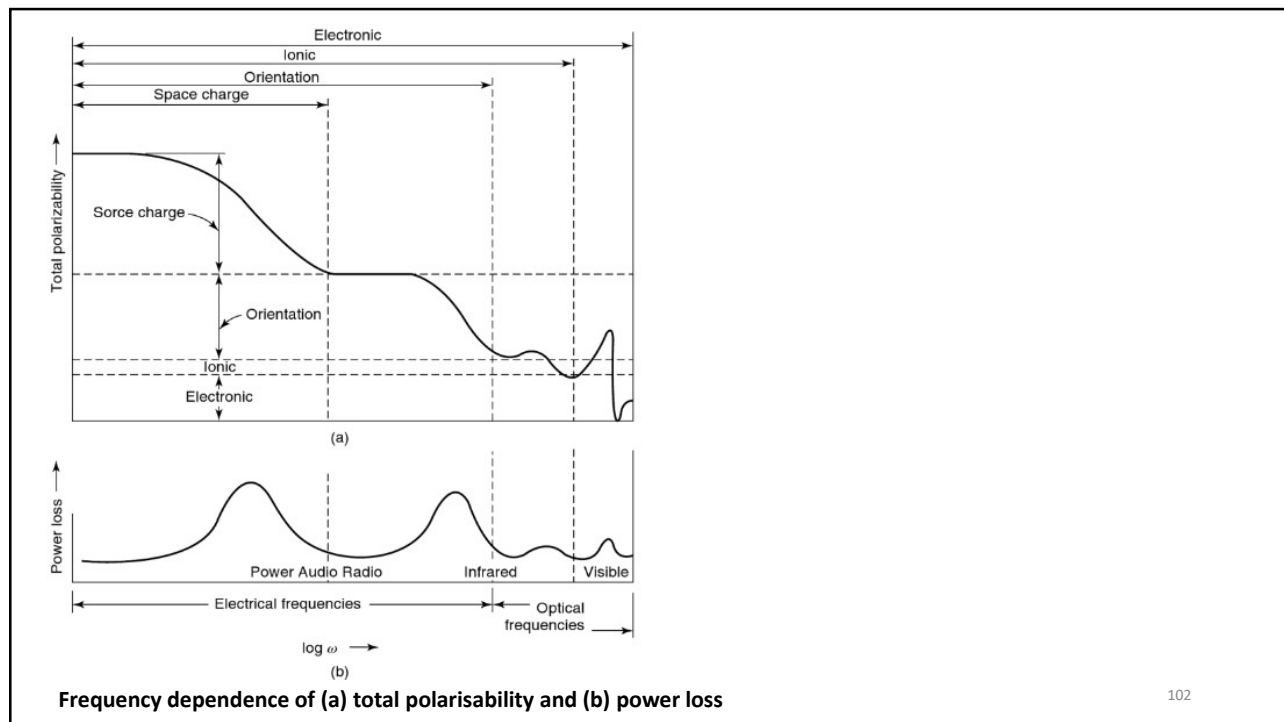
Approximate ion displacements in the cubic–tetragonal distortion in $BaTiO_3$

1. Raengthon, N., McCue, C., & Cann, D. P. (2016). Relationship between tolerance factor and temperature coefficient of permittivity of temperature-stable high permittivity BaTiO3–Bi (Me) O3 compounds. *Journal of Advanced Dielectrics*, **6(01), 1650002**.
2. Brehm, J. A., Bennett, J. W., Schoenberg, M. R., Grinberg, I., & Rappe, A. M. (2014). The structural diversity of AB S3 compounds with d 0 electronic configuration for the B-cation. *The Journal of Chemical Physics*, **140(22), 224703**.
3. Table: https://jaramillo.mit.edu/modified-goldschmidt-tolerance-factor-calculator-abx3-compounds
4. Hoshina, T., Kigoshi, Y., Hatta, S., Takeda, H., & Tsurumi, T. (2009). Domain contribution to dielectric properties of fine-grained BaTiO3 ceramics. *Japanese Journal of Applied Physics*, **48(9S1), 09KC01**.
5. Richerson, D. W., & Lee, W. E. (2018). *Modern ceramic engineering: properties, processing, and use in design*. **CRC press**.

99

The ionic displacement in the c-axis direction initiates the ferroelectric dipole. Thus, it enhances the tetragonality (c/a) and creates large spontaneous polarization. However, there is an optimum oxygen pressure range to enhance the dielectric and ferroelectric of the $BaTiO_3$. With c-axis becoming relatively shorter, the dipole moment and the polarizability of the samples are reduced.

BaTiO$_3$ unit cell (.............................) (b) looking at one face, exhibiting the displacement of Ti^{4+} and O^{2-} ions from the center of the face

100

Directions of spontaneous polarization in the (a) tetragonal, (b) orthorhombic and (c) rhombohedral phase. Angles between polarization direction '0' and its symmetry equivalent ones are indicated.

Marton, Physical review. B, Condensed matter 81(14), 2010

101

18

**Frequency dependence of (a) total polarisability and (b) power loss**

102

The paraelectric to ferroelectric phase transition

In some perovskites containing Ti or Nb on the B site ($BaTiO_3$, $PbTiO_3$, $KNbO_3$), a phase transition from a paraelectric cubic structure to a lower symmetry phase (tetragonal) with appearance of spontaneous polarization occurs at a critical temperature T_C (Curie temperature).
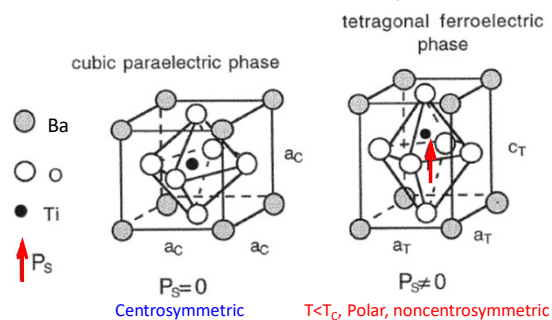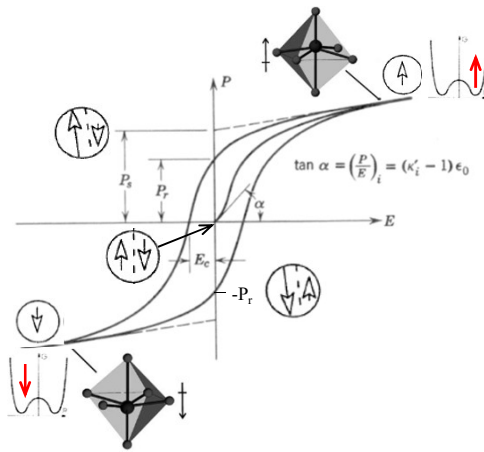

Spontaneous strain: $(c_T-a_T)/a_C \approx c_T/a_c - 1$

| Compound	T_C (°C)	P_S ($\mu C/cm^2$)	$Q_{c\text{-}t}$ (J/mol)	c_T/a_T-1	Δz(Ti) (pm)
$BaTiO_3$	125	26	197	1%	120
$PbZr_{0.5}Ti_{0.5}O_3$ (PZT)	380	40-50	-	2.5%	-
$PbTiO_3$	495	81	4815	6.5%	300
$KNbO_3$	435	30	796	-	-

$$T_C = 2 \times 10^4 \, (\Delta z)^2$$

103

19
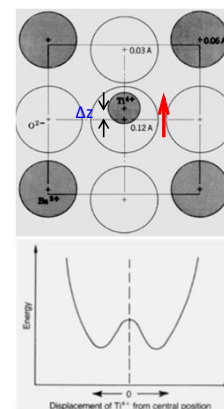
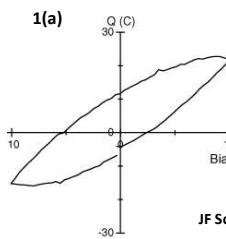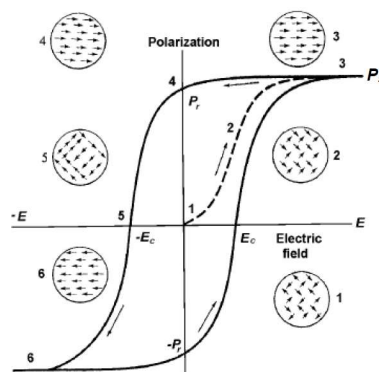Ferroelectric hysteresis loop and polarization switching

P_S: saturation (spontaneous) polarization
P_R: remanent polarization
E_C: coercive field
The slope of the initial polarization curve gives the dielectric constant

Ideally $+P_R = -P_R$ and $+E_C = -E_C$

$$\tan \alpha = \left(\frac{P}{E}\right)_i = (\kappa_i' - 1)\epsilon_0$$
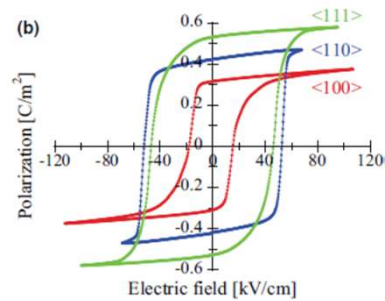
104

Hysteresis loop: the fingerprint of ferroelectricity

JF Scott, J. Phys.: Condens. Matter 20 (2008)

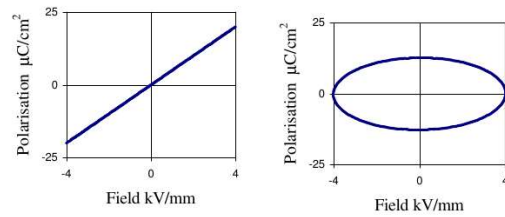Q = 2P_rA [saturated ferroelectric, ideally]
Q = 2P_rA + σEAt [in real situations]
Q= σ EAt [linear lossy dielectric]

Switched charge Q versus applied electric voltage V is not the same as polarisation-electric field (P–E) loops

If your `hysteresis loops' look like figure 1(a), please do not publish them. Publish data that are saturated and have a region in Q versus V that is concave. Bananas are not ferroelectric, and it is easy to be misled by closed Q(V) loops.

105

Q = 2P$_r$A [saturated ferroelectric, ideally]
Q = 2P$_r$A + σEAt [in real situations]
Q= σ EAt [linear lossy dielectric]

Switched charge Q versus applied electric voltage V is not the same as polarisation-electric field (P–E) loops

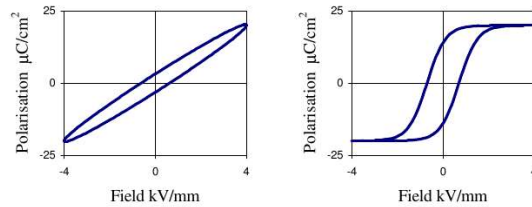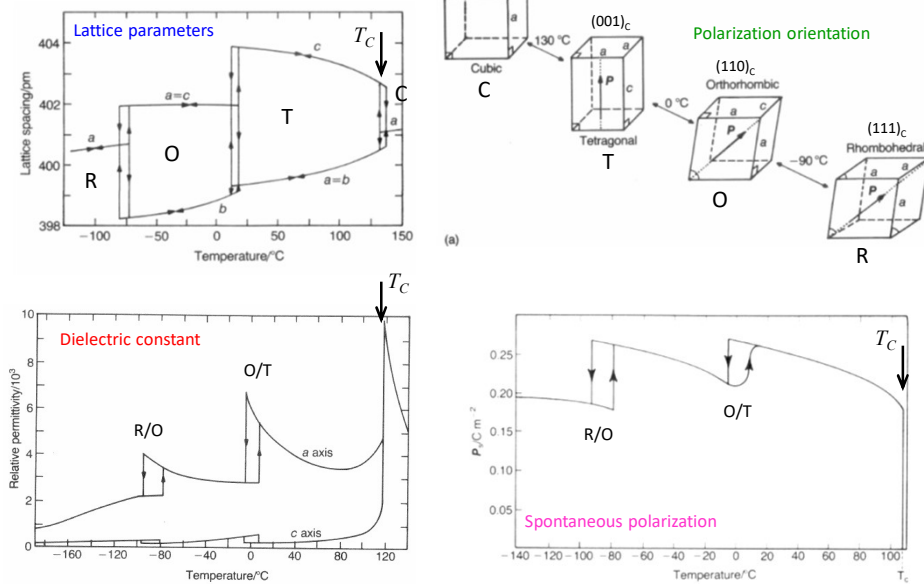Figure 1a): Ideal linear capacitor response   Figure 1b) Ideal resistor response

Figure 1c): Lossy capacitor response   Figure 1d): Non-linear ferroelectric response
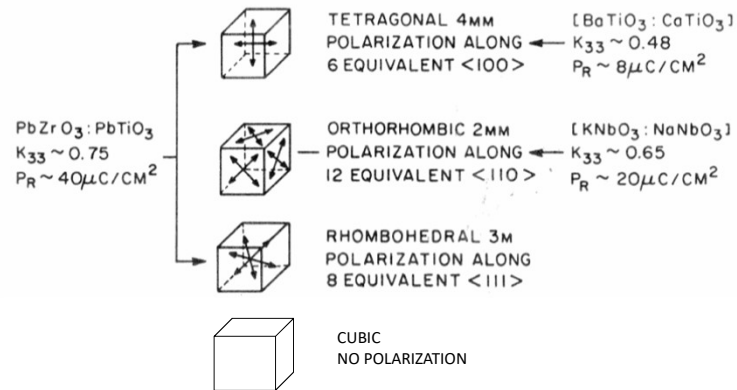
106

Phase transitions in barium titanate

107

21

Phase transitions in ferroelectric perovskites

POSSIBLE ORIENTATION STATES IN PEROVSKITES

$PbZrO_3 : PbTiO_3$
$K_{33} \sim 0.75$
$P_R \sim 40 \mu C / CM^2$

TETRAGONAL 4MM
POLARIZATION ALONG
6 EQUIVALENT <100>

$[BaTiO_3 : CaTiO_3]$
$K_{33} \sim 0.48$
$P_R \sim 8 \mu C / CM^2$

ORTHORHOMBIC 2MM
POLARIZATION ALONG
12 EQUIVALENT <110>

$[KNbO_3 : NaNbO_3]$
$K_{33} \sim 0.65$
$P_R \sim 20 \mu C / CM^2$

RHOMBOHEDRAL 3M
POLARIZATION ALONG
8 EQUIVALENT <111>

CUBIC
NO POLARIZATION

Polymorphic phase transition (PPT) in ferroelectrics are determined by:
- temperature change;
- external electric field;
- external stress;

108